Role of α-Helix Seven of *Bacillus thuringiensis* Cry1Ab δ-Endotoxin in Membrane Insertion, Structural Stability, and Ion Channel Activity†

Edwin P. Alcantara,‡ Oscar Alzate,§,⊥,|| Mi K. Lee,⊥ April Curtiss,⊥ and Donald H. Dean*,‡,§,⊥

Department of Entomology, Biophysics Program, and Department of Biochemistry, The Ohio State University, Columbus, Ohio 43210 USA, and Universidad Pontificia Bolivariana, Medellín, Colombia

Received September 21, 2000; Revised Manuscript Received January 2, 2001

ABSTRACT: Domain I of the Cry1Ab insecticidal toxic protein has seven α-helices and is considered to be involved in the ion channel activity. While other α-helices, particularly α-4 and α-5, have been extensively explored, the remaining α-helices have been slightly studied. Site-directed mutagenesis was used to generate mutations throughout sequences encoding the α-helix 7 to test its role in ion channel function. Every amino acid residue in α-helix 7 was mutated to alanine. Most resultant proteins, e.g., D225A, W226A, Y229A, N230A, R233A, R234A, D242A, and F247A yielded no protoxin or were sensitive to degradation by trypsin or *Manduca sexta* midgut juice. Other mutant proteins, R224A, R228A, and E235A, were resistant to degradation to the above proteases but were 8, 30, and 12 times less toxic to *M. sexta*, respectively, than the wild-type Cry1Ab. Circular dichroism spectroscopy indicated a very small change in the R228A spectrum, while R224A and E235A display the same spectrum as the wild-type protein. These three mutant proteins showed little differences from Cry1Ab when analyzed by saturation binding and competition binding kinetics with ^{125}I-labeled toxin or by surface plasmon resonance to *M. sexta* brush border membrane vesicles. More conservative amino acid substitutions were introduced into α-helix 7 residues: R228K, F232Y, E235Q, and F247Y. In comparison with wild-type Cry1Ab, mutant proteins R228K, F232Y, E235A, and E235Q selectively discriminate between K^+ and Rb^+, while R224A and R228A had reduced inhibition of short-circuit current for both ions, when analyzed by voltage clamping of *M. sexta* midguts.

The Bt proteins (Bt δ-endotoxins)[1] have no toxic effects on higher organisms but are highly toxic to susceptible insects, which makes the toxins ideal for integration into insect pest management schemes. In the case of the Cry1 family of δ-endotoxins, upon ingestion by a susceptible insect, the parasporal inclusions (∼130-kDa protein in the protoxin state) are solubilized and activated into a 65-kDa toxin by the highly alkaline environment and the insect midgut proteases (*1*−*3*). After binding to receptors in the gut (*4*), the toxin forms cation permeable pores that destroy the large transepithelial potential. The loss of this driving force eventually gives rise to an increase in intracellular pH and larval death (*5*). The Bt toxins are classified into several major families of Cry toxins (*6*). Many of the lepidopteran specific toxins fall into the Cry1A family. The 3D structure of Cry1Aa, as revealed by X-ray crystallography (*7*), is very similar to the structure of the Cry3A toxin (*8*). Cry1A type toxins are believed to have similar structure as Cry1Aa because of the high homology in amino acid sequence (*6*, *9*). The α-helical domain I, when physically separated from the whole protein, is capable of pore formation as shown by planar lipid bilayer studies (*10*, *11*); however, the ionic conductance of this pore does not equal that of the whole toxin. It is also known that domain III affects ion transport across the midgut membrane of susceptible insects (*12*−*14*). Several mutational studies in domain I have been reported. Total loss of toxicity was observed with some mutations introduced in α-helix 5 of Cry1Ac (*15*) and with cysteine mutations in the same region on Cry1Ab (*16*). Another study reported loss of irreversible binding and toxicity in Cry1Ab when mutations were introduced within the region spanning α-helix 3 and α-helix 4 (*17*). Mutations were also introduced in α-helix 6 of Cry1Ac but no substantial loss of toxicity was reported (*18*). α-helix 7 is located in the crucial junction between domain I and II (*7*, *8*). Some studies on the possible role of α-helix 7 in the mode of action is based on experiments with synthetic peptides (*19*, *20*). It was reported that the peptide mimicking α-helix 7 could possibly function as a binding sensor of domain I which assumes that the toxin

† This work was supported by a NIH grant (R01 AI 29092) to D.H.D. E.P.A. is a recipient of a Rockefeller foundation fellowship and is now with the University of the Philippines, Los Baños. O. Alzate was a fellow supported by the Colombian Institute for the Advancement of Science (COLCIENCIAS).

* To whom correspondence should be addressed. Telephone: (614) 292-8829. Fax: (614) 292-6773. E-mail: dean.10@osu.edu.

‡ Department of Entomology, The Ohio State University.

§ Biophysics Program, The Ohio State University.

⊥ Department of Biochemistry, The Ohio State University.

|| Universidad Pontificia Bolivariana.

[1] Abbreviations: BBMV, brush border membrane vesicles; $B_{max,i}$, number of irreversible binding sites; Bt, *Bacillus thuringiensis*; EDTA, ethylenediaminetetraacetic acid; HEPES, 4-(2-hydroxyethyl)-1-piperazine ethanesulfonic acid; I_{sc}, short circuit current; k_1, association rate; k_{-1}, dissociation rate; K_D, apparent dissociation constant; K_{com}, apparent dissociation constant from competitive binding; k_{obs}, rate of irreversible binding; LC_{50}, median lethal concentration; CAPS, 3-[cyclohexylamino]-1-propanesulfonic acid; HBS, 10 mM HEPES, pH 7.4, 150 mM NaCl, and 3.4 mM EDTA; SPR, surface plasmon resonance.

10.1021/bi0022240 CCC: $20.00
Published on Web 01/30/2001

undergoes major conformational change after receptor binding. Chandra et al. (*21*) have replaced a nine-amino acid region on the C-terminal end of α-helix 7 of Cry1Ac with a similar region from diphtheria toxin. They have reported that this α-helix is involved in ion transport and toxicity, as determined by voltage clamping experiments in black lipid membranes and insect bioassays. To the best of our knowledge, no work has been done to determine the functional properties of specific residues in α-helix 7 of the Cry1Ab toxin using membranes from isolated midguts of tobacco hornworm, *Manduca sexta*. Therefore, in the present work, we have introduced several point mutations in the α-helix 7 of Cry1Ab by site-directed mutagenesis to determine the role of charged and hydrophobic residues in membrane binding and insertion, structural stability, and ion channel activity. The results of our study show that substitution of alanine for most residues in α-helix 7 of Cry1Ab results in protoxins that are sensitive to protease digestion, suggesting their involvement in maintaining structural stability of the toxin. A very interesting observation is that certain residues in α-helix 7 affect binding affinity and toxicity and might be involved in ion channel activity.

MATERIALS AND METHODS

Site-Directed Mutagenesis. The template *cry1Ab9*−*033b* (*22*), hereafter referred to as *Cry1Ab*, was used for the mutations. The oligonucleotides were provided by Sandoz Agro, Inc. The mutagenesis kit (Muta-Gene Phagemid in vitro Mutagenesis) was purchased from Bio-Rad. Site-directed mutagenesis was carried out by the Kunkel method (*23*). Point mutations were generated by hybridizing the mutagenic oligonucleotide with the uracylated *cry1Ab* single stranded template. After synthesis of double strand DNA, the selection of mutants was facilitated by transformation in *Escherichia coli* MV1190. Mutants were confirmed by single stranded DNA sequencing (*24*). Reagents for DNA sequencing were purchased from United States Biochemicals.

Toxin Preparation. A single colony of *E. coli* MV1190 containing the mutant *cry1Ab* gene was grown in 500 mL of Terrific Broth Medium (*25*) for 48 h at 37 °C under vigorous agitation (250 rpm). Pelleted cells were resuspended in lysis buffer (50 mM Tris, pH 8.0, 50 mM EDTA, 15% sucrose, and 10 μg/mL lysozyme) and incubated overnight with agitation at 37 °C. Purification of inclusion bodies, protoxin extraction, and toxin activation was carried out as described previously (*26*). The quality of the toxins was deemed to be purified to homogeneity as analyzed by 12% SDS−PAGE (*27*). Toxin concentrations were determined by Coomassie protein assay reagent (Pierce).

Insect Gut Juice Assay. Gut juice was collected from fifth instar *M. sexta* larvae (*22*). Fresh gut juice was centrifuged to remove any particulate. The supernatant was stored at −70 °C until use. For the assay, 1 μL of gut juice was mixed with 5 μg of Cry1Ab protoxin to a final volume of 10 μL of carbonate−bicarbonate buffer, pH 9.5. Incubation of all the samples was done at 37 °C for 1 h.

Thermolysin Digestion. Thermal stability of protease stable mutant toxins were further analyzed by thermolysin digestion as previously described (*26*). Briefly, 30 μg toxin was incubated with thermolysin at various temperatures for 20 min in buffer containing 50 mM Tris, pH 9.5, and 10 mM $CaCl_2$. The reaction was terminated by adding 20 mM EDTA (final concentration). Stability of mutants from thermolysin digestion was confirmed by SDS−PAGE.

Iodination of Toxins. Twenty-five micrograms of each toxin was labeled with 1 mCi of ^{125}I (specific activity of stock ^{125}I was ∼17 Ci/mg, Dupont) (*22*). The specific activity of each toxin was determined by cutting out the toxin bands from the SDS−PAGE gel and counting the radioactivity with a gamma counter (Beckman). The specific activity of the toxins was about 50 cpm/fmol (23 μmol ^{125}I/mol toxin).

Receptor Binding Assays. Brush border membrane vesicles (BBMV) were prepared from fifth instar *M. sexta* midguts as described (*28*). Competition binding was performed as previously described (*29*). The dissociation constant (K_{com}) (*30*) was calculated from competition binding by using the PRISM computer program (GraphPad, Inc). The rate of irreversible binding (k_{obs}) and the number of binding sites ($B_{max,i}$) were calculated from association and saturation assays of irreversible binding, respectively (*31*).

The BIAcore 2000 surface plasmon resonance (SPR) machine (Pharmacia) was used to measure real time binding kinetics of Cry1Ab mutant toxins on biotinylated *M. sexta* BBMVs. The method of Masson et al. (*32*) was followed with minor modifications to biotinylate the purified BBMVs. A 1:50 (wt/wt) mixture of *N*-biotin-phosphatidylethanolamine (Avanti Polar Lipids) and purified BBMVs were sonicated in a water bath sonicator for 5 min followed by 1-h centrifugation at 100000*g*. The high-speed centrifugation was repeated once more after the pelleted biotinylated BBMVs were resuspended in HBS buffer (10 mM HEPES, pH 7.4, 150 mM NaCl, and 3.4 mM EDTA). The final suspension of biotinylated BBMV was centrifuged at 3000*g* for 5 min to remove debris. The concentration of the biotinylated BBMVs was adjusted to 1 mg/mL and stored at −70 °C. The CM5 sensor chip (Pharmacia) that houses four flow cells was immobilized with 6 μg of rabbit antibiotin (Cortex Biochem) diluted in 20 mM ammonium acetate buffer at pH 4.5. After a 40 min wash, 100 μg of biotinylated BBMV was added to the immobilized antibiotin in all the flow cells. The binding response was measured by loading 50 μL of a 2 μM solution of each toxin per flow cell and monitored on-line. The binding affinity, K_D (M), was calculated as the ratio of dissociation rate, k_{-1} (s^{-1}), and association rate, k_1 (M^{-1} s^{-1}). In all the experiments, HBS buffer was used with a flow rate of 5 μL/min. All toxins were predialyzed in the same buffer. After each experiment, the BBMV with bound toxin was removed by flushing the flow cells with 25 μL of CAPS buffer, pH 11.0, followed by 25 μL of HBS with 0.1% Triton X-100. The sensor was primed with HBS buffer before the next binding experiment.

Bioassays. The median lethal concentrations (LC_{50}) of the toxins were estimated by performing diet surface contamination assays. Three-day-old *M. sexta* larvae were confined in sterile dishes containing solidified artificial diet (BioServ) surface contaminated with activated toxin. Five to six toxin concentrations were prepared for each assay. Twenty larvae were used for each concentration. Mortalities were scored after 5 days. The LC_{50} for each toxin was calculated by Probit analysis (*33*).

Electrophysiology. Short circuit current (I_{sc}) inhibition by activated toxin in *M. sexta* midgut was measured by voltage clamping (*34*). The apparatus used to short-circuit the midgut

was a DVC-1000 voltage/current clamp (World Precision Instruments). On-line data acquisition was carried out by connecting the voltage clamp setup to an analog/digital converter. The anterior portion of early fifth instar *M. sexta* midguts were used for the measurements. I_{sc} was measured from tissue having an apparent surface area of about 0.44 cm^2. The hemolymph and luminal sides of the tissue were constantly bathed in 4 mL of vigorously oxygenated KCl buffer, pH 8.0 (*34*). When the transepithelial potential was about −150 to −200 mV (open circuit), the tissue was clamped to a holding potential of 0 mV (short circuit). After 30 min, activated toxin (1 nM) was added to the lumen side of the tissue. Recorded I_{sc} data was normalized to % I_{sc} remaining. Toxin effect was expressed as the normalized slope of the I_{sc} drop (% I_{sc} remaining min^{-1} cm^{-2}). The experiment for each toxin was repeated three times. To determine the effect of the point mutations on the ionic selectivity of each mutant toxin, the actively transported K^+ was replaced with an equimolar concentration of RbCl. All other experimental conditions were the same as described above. Mutants showing altered I_{sc} inhibition were further analyzed by voltage clamping with increasing amounts of toxin in a fixed molar concentration of KCl and RbCl buffer.

Statistical Analysis. One way analysis of variance (ANOVA) was used to determine significant difference in treatment means at $\alpha = 0.05$. Comparison between wild type and each mutant treatment means was carried out with Bonferroni *t*-test (*33*). Mutants are significantly different from wild type when $P < 0.05$. LC_{50} estimates are declared significantly different from wild type when their 95% fiducial limits do not overlap.

Secondary Structure Analysis. Purification of trypsin-activated toxins for circular dichroism (CD) analysis was done by high-pressure liquid chromatography (HPLC) utilizing a Waters 625 photodiode array detector with the Bio-Gel SEC 30-XL 300 × 7.8 mm size exclusion column (Bio-Rad). The toxin fraction was eluted with 5 mM KH_2PO_4/K_2HPO_4 buffer, pH 7.4, that was prefiltered through a 20 μm filter paper (Millipore). The toxin fractions were concentrated in 2-mL Centricon50 concentrator tubes (Amicon). Proteins were purified to homogeneity as determined by SDS−PAGE electrophoresis. The spectra were collected in a AVIV CD2 spectropolarimeter at room temperature with a 1-cm path length quartz cell (Hellma) containing 3 mL of solution [30 μg toxin in 3 mL of Milli-Q water (Millipore)] scanning from 250 to 200 nm at 1.0 nm steps. Data were based on the average of 10 scans.

RESULTS

Effect of Mutations in α-Helix 7 on Structural Stability of Cry1Ab. Trypsin digestion, exposure to *M. sexta* gut juice, and thermal analysis with Thermolysin were used to determine the structural stability of mutant toxins. Five of the 11 mutations introduced to the DNA sequence encoding α-helix 7 either failed to produce protoxin, or if protoxin was expressed in *E. coli*, it was degraded by trypsin in vitro. Alanine substitutions in positions D225, W226, and D242 produced no detectable amount of protoxin. Mutant proteins N230A and R234A produced protoxin but did not produce a stable 65-kDa toxin after treatment with trypsin. Mutants R224A, R228A, Y229A, R233A, E235A, and F247A produced the protoxin and trypsin resistant toxin comparable to the wild type. The stability of these trypsin resistant mutant toxins was further tested with undiluted *M. sexta* gut juice. This assay mimics in vivo enzymatic conditions (i.e., the array of proteases present) and is assumed to be harsher than midgut conditions in temperature and duration (37 °C, 1 h). The assay showed that mutant toxins Y229A, R233A, and F247A were less stable as compared to the wild type as revealed by SDS−PAGE analysis (data not shown). Three mutant toxins (R224A, R228A, and E235A) were found to be stable under the conditions defined for the proteolytic assays and were also thermostable as revealed by thermolysin assay and SDS−PAGE (Figure 5). The position of the wild-type residues in α-helix 7 that produced stable alanine mutants is shown in Figure 1. Protease digestion assay results suggest that the α-helix 7 is critical for the structural stability of the whole toxin; therefore, we introduced more conservative mutations in α-helix 7 (W226F, R228K, Y229F, F232Y, E235Q, F247Y, and Y250F) to avoid producing structural instability to the toxin. As with the wild-type toxin, the conservative mutants except W226F were resistant to trypsin and *M. sexta* gut juice assays (data not shown).

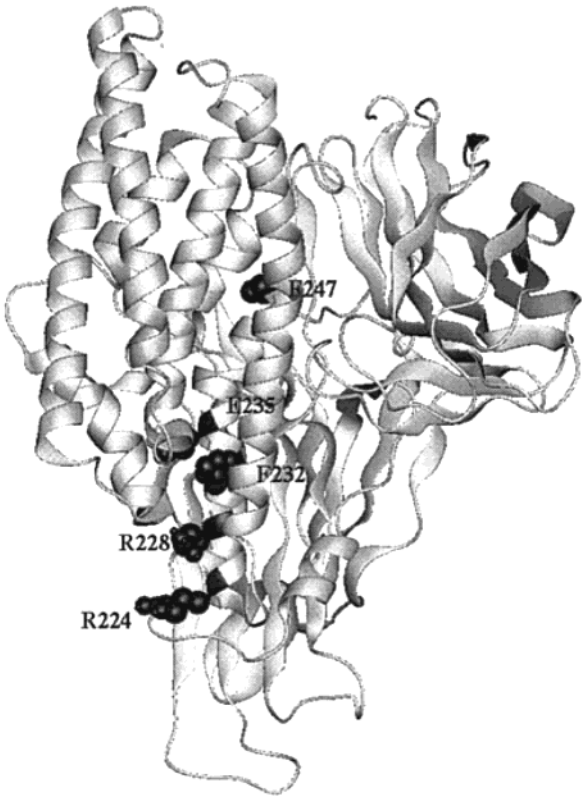

FIGURE 1: Molecular graphics depicting the positions of R224, R228, F232, E235, and F247 in α-helix 7 of Cry1Ab. The atomic coordinates of Cry1Aa obtained from Brookhaven Protein Data Bank were used as "template" to construct the structural model for Cry1Ab. Molecular simulations were done using the program Quanta in a Silicon Graphics Indigo (SGI) workstation.

Effect on Secondary Structure. Figure 2 shows the CD spectra of the wild type, R224A, and R228A mutant toxins in the region between 200 and 250 nm. Two distinct absorption minima at 210 and 220 nm were observed for the wild type toxin. Mutant toxins showed almost exactly the same CD spectrum as Cry1Ab, particularly R224A, whose spectrum can be overlapped with the Cry1Ab CD spectrum. There is probably a small rearrangement in the

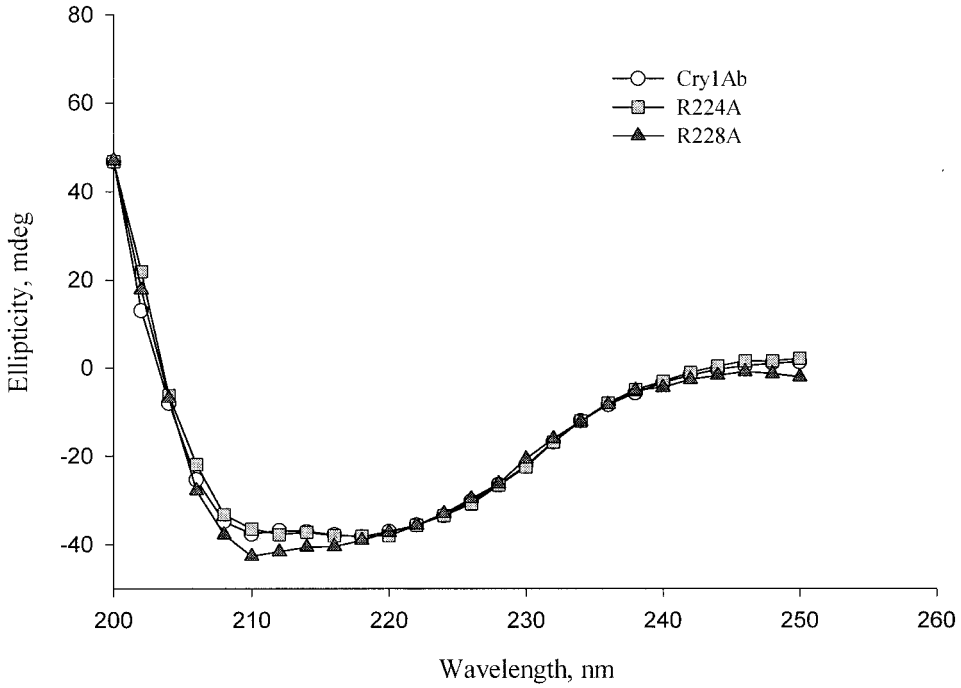

FIGURE 2: Secondary structure analysis by circular dichroism spectra of Cry 1Ab toxins. (○, wild type; solid gray square, R224A; solid gray triangle, R228A).

Table 1: Binding and Toxicity Parameters for Cry1Ab and Alanine Mutant Toxins[a]

				I_{sc} inhibition[e] (% I_{sc} remaining min^{-1} cm^{-2})		
toxin	K_{com}[b] (nM)	$B_{max,i}$[c] (fmol/μg)	K_{obs}[d] (min^{-1})	KCl	RbCl	LC_{50}[f] (ng/cm^2)
Cry1Ab	12.51(0.99)	2.87(0.88)	0.20 (0.02)	17.23 (0.37)	17.95 (1.82)	57.49 (49.11−68.91)
R224A	12.66(0.41)	1.02(0.40)	0.23 (0.07)	12.36 (1.50)	13.88 (1.19)	182.6(155.4−211.7)
R228A	14.85(2.49)	0.37(0.18)	0.57 (0.16)	2.29 (0.42)	1.91 (0.58)	766.6 (634.4−876.8)
E235A	31.89(6.76)	3.43(0.59)	0.99 (0.41)	6.04 (0.42)	18.92(0.43)	251.77 (229.9−283.1)

[a] Underlined values are significantly different from wild type ($P < 0.05$). Significant difference in means determined by Bonferroni *t*-test. Values given in parentheses are standard deviations unless otherwise indicated. [b] K_{com} dissociation constants determined by heterologous competition binding assays of 2 nM I^{125}-labeled wild-type toxin with 0−1000 nM unlabeled mutant toxins. [c] $B_{max,i}$, number of irreversible binding sites. [d] k_{obs}, rate of irreversible membrane binding of 0.5 nM I^{125} labeled toxins in *M. sexta* brush border membrane vesicles. [e] I_{sc} inhibition, drop in short circuit current after toxin treatment of voltage clamped midguts. Initial I_{sc} is 150 ± 45 μA. [f] LC_{50}, median lethal concentration with 95% confidence intervals.

R228A conformation, as shown at the 222 nm position. However, the digestion assays, show that the suggested conformational changes are not big enough to alter the native conformation of the R228A toxin. Mutant toxins R228K, F232Y, E235A, E235Q, and F247Y showed CD spectra similar to the wild type (data not shown).

Toxicity, Receptor Binding, and Membrane Insertion. Mutant toxins R224A, R228A, and E235A were significantly less toxic than the wild type (LC_{50} = 57.49 ng/cm^2) in larval bioassays (Table 1). The decrease in toxicity was 3 times in R224A (LC_{50} = 182.6 ng/cm^2), 4 times in E235A (LC_{50} = 251.77 ng/cm^2), and up to 13 times in R228A (LC_{50} = 766.6 ng/cm^2). However, the introduction of more conservative mutations in α-helix 7 did not significantly reduce the toxicity below the wild-type level (Table 2). The toxicities of mutant toxins R228K (52.29 ng/cm^2), F232Y (54.13 ng/cm^2), E235Q (74.12 ng/cm^2), and F247Y (49.84 ng/cm^2) were similar to wild type.

Binding assays with I^{125} labeled toxins were conducted to analyze toxin−receptor interactions. The binding parameter estimated from the competition curves (Table 1) showed that E235A had a significantly larger K_{com} (31.89 nM) than the wild type (K_{com} = 12.51 nM). R224A (K_{com} = 12.66 nM) and R228A (K_{com} = 14.85) were not different from the wild type. The saturation assay for irreversible binding revealed a significant change in the number of irreversible binding sites for R228A ($B_{max,i}$ = 0.37 fmol/μg). R224A ($B_{max,i}$ = 1.02 fmol/μg) and E235A ($B_{max,i}$ = 3.43 fmol/μg) were not significantly different from the wild-type toxin ($B_{max,i}$ = 2.87 fmol/μg). The rate of irreversible membrane binding (k_{obs}), estimated from the association assay of irreversible binding, shows that k_{obs} for R224A (0.23 min^{-1}), R228A (0.57 min^{-1}), and E235A (0.99 min^{-1}) were not significantly different from wild-type toxin (Table 1). All binding parameters estimated for R228K, F232Y, E235Q, and F247Y were also not significantly different from wild type (Table 2).

Binding assays with SPR were used to compare the real time binding kinetics of mutant toxins with wild-type Cry1Ab toxin. The estimated binding parameters for mutant toxins are shown in Table 3. Association rates (k_1) were not significantly different among all toxins. However, the dissociation rate (k_{-1}) of R224A (6.6×10^{-4}), R228A (7.3×10^{-4}), E235A (1.7×10^{-3}), and R228K (5.8×10^{-4}) were significantly slower than wild type (2.1×10^{-4}). The affinity

Table 2: Binding and Toxicity Parameters for Cry1Ab and Conservative Mutant Toxins[a]

toxin	K_{com}[b] (nM)	$B_{max,i}$[c] (fmol/μg)	K_{obs}[d] (min^{-1})	I_{sc} inhibition[e] (% I_{sc} remaining min^{-1} cm^{-2}) KCl	RbCl	LC_{50}[f] (ng/cm^2)
Cry1Ab	0.55(0.08)	3.09(0.43)	0.055(0.01)	16.00(0.1)	16.8 (1.71)	57.49(49.11−68.91)
R224K	1.40(0.60)	2.57(0.50)	0.063(0.01)	16.30(2.4)	7.33(1.92)	52.29(36.11−74.44)
*F*232Y	0.53(0.02)	3.00(0.73)	0.051(0.01)	19.00(2.9)	10.23(1.7)	54.13(38.44−81.08)
E235Q	0.77(0.20)	2.57(0.55)	0.091(0.01)	14.50(1.5)	7.39(1.4)	74.12(55.28−97.90)
F247Y	0.36(0.07)	3.20(0.81)	0.052(0.01)	19.50(2.5)	16.00(1.48)	49.84(23.88−73.76)

[a] Values estimated from all binding and voltage clamping experiments are not significantly different from wild type ($P > 0.05$). [b] K_{com}, dissociation constants determined by homologous competition binding of 2 nM of I^{125}-labeled wild-type toxin. [c] $B_{max,i}$, number of irreversible binding sites. [d] k_{obs}, rate of irreversible binding. [e] I_{sc}, drop in short circuit current after toxin treatment of voltage clamped midguts. Initial I_{sc} is 150 ± 45 μA. [f] LC_{50}, median lethal concentration, values in parentheses are 95% confidence limits.

Table 3: Binding Parameters for Cry1Ab and Mutant Toxins Measured by SPR

toxin	$k_1 \times 10^3$ ($M^{-1}s^{-1}$)[a]	$k_{-1} \times 10^{-4}$ (s^{-1})[b]	$K_D \times 10^{-8}$ (M)[c]	n[d]
Cry1Ab	7.56 ± 2.74	2.10 ± 0.22	2.91 ± 0.71	3
R224A	9.47 ± 1.24	6.60 ± 0.64	7.00 ± 0.94	3
R228A	7.89 ± 1.02	7.30 ± 2.20	9.20 ± 1.70	3
R228K	8.14 ± 0.93	5.80 ± 0.81	7.20 ± 1.80	2
E235A	9.59 ± 1.28	17.00 ± 0.07	18.00 ± 2.10	2
E235Q	8.04 ± 1.99	4.10 ± 0.19	5.10 ± 1.90	2

[a] k_1, association rate. [b] k_{-1}, dissociation rate. [c] K_D, affinity (k_{-1}/k_1). [d] n, number of replicates.

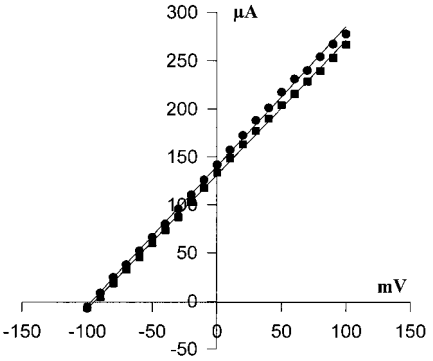

FIGURE 3: Current-voltage plot of short circuited fifth instar *M. sexta* midgut in KCl (●) and RbCl (■) buffers. Each curve is an average of three replicates. The slope of the curve is equal to the midgut permeability to the ion producing the short circuit current (I_{sc}).

(K_D) of R228A (9.2×10^{-8} M) and E235A (1.8×10^{-7} M) were significantly weaker than wild type (2.9×10^{-8}). The K_D of R224A (7.0×10^{-8}), R228K (7.2×10^{-8}), and E235Q (5.1×10^{-8}) were similar to wild type. The significance of these binding results is that the K_D values (Table 3) do not necessarily correlate with toxicity (Table 2). This is expected since K_D obtained from SPR does not consider either the rate of insertion into the membrane or the ion transport capability of the toxin. We believe this indicates a complex role for these residues in the mechanism of action, related to ion channel function.

Ion Channel Activity. Voltage clamp was used to analyze the ability of mutant toxins to form ion channels in the insect midgut and to detect changes in the ion selectivity of the mutant proteins. Figure 3 shows that the permeability (σ) of untreated *M. sexta* midgut to K^+ ($\sigma = 1.39$ μA/mV) and Rb^+ ($\sigma = 1.45$ μA/mV) are similar. The time course of I_{sc} inhibition by the toxin in midgut vesicles from *M. sexta* in buffers containing KCl and RbCl is shown in Figure 4, panels

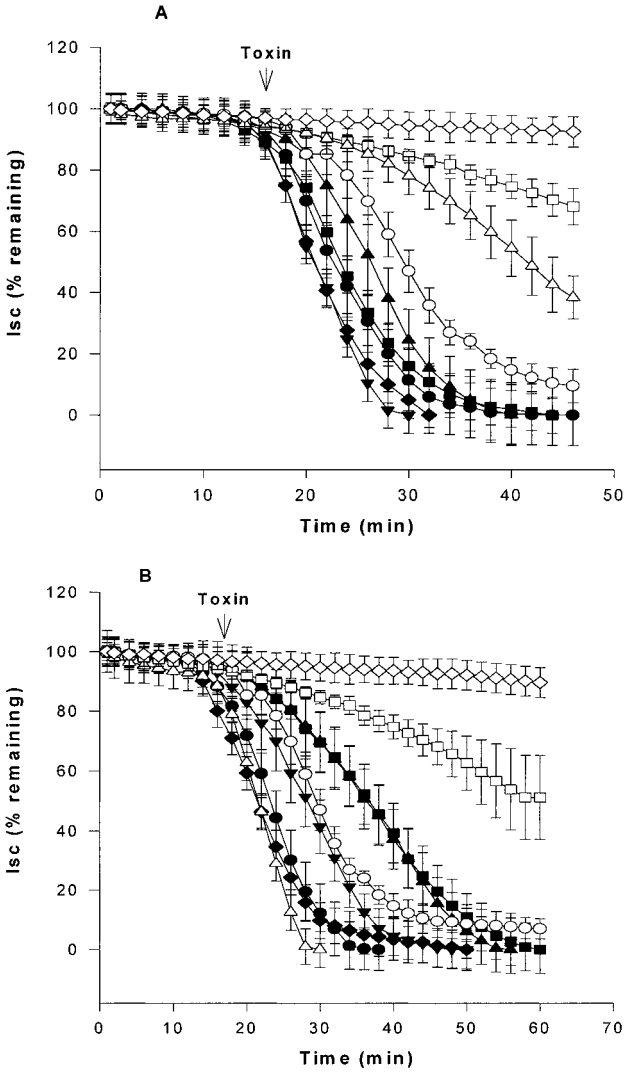

FIGURE 4: Time course of short circuit current inhibition (I_{sc}) of *M. sexta* midgut by 1 nM Cry1Ab and mutant toxins. Each curve is an average of three experiments. The average initial I_{sc} was about 150 μA/cm^2. (A) With KCl in the chamber buffer. (B) With RbCl in the chamber buffer. The vertical bar on each data point is the standard deviation. (●, wild type; ○, R224A; □, R228A; △, E235A; ■, R228K; ▼, F232Y; ▲, E235Q; ◆, F247Y; ◇, untreated midgut).

A and B, respectively. The same concentration (1.0 nM) was used for all toxins. Cry1Ab toxin reduced active K^+ and Rb^+ transport to 50% of initial midgut I_{sc} levels in about 22 min in both KCl and RbCl buffers, corresponding to an average I_{sc} inhibition rate of −16.61% min^{-1} cm^{-2} and −17.37% min^{-1} cm^{-2}, respectively (Tables 1 and 2). A longer time

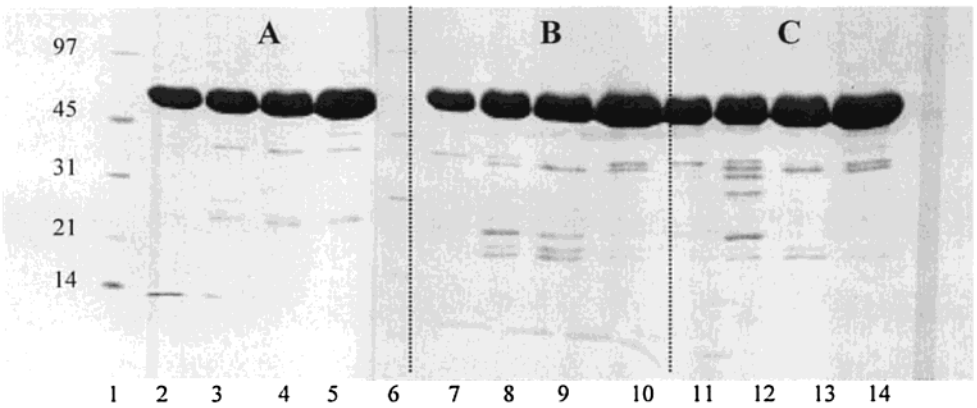

FIGURE 5: Thermolysin digestion profile of Cry1Ab wild type and mutant toxins. Lanes 1 and 6, low range molecular weight markers; lanes 2, 7, and 11 contain wild-type toxin; lanes 3, 8, and 12 contain R224A; lanes 4, 9, and 13 contain R228A; lanes 5, 10, and 14 contain E235A. The trypsin-activated toxins were digested with thermolysin at 37 (panel A), 58 (panel B), and 65°C (panel C) for 20 min.

was needed to achieve the same effect by mutant R224A (30 min) and R228A (more than 50 min) in both KCl (Figure 4, panel A) and RbCl (Figure 5, panel B) buffers. The I_{sc} inhibition rate of R224A (Table 1) in KCl (-12.36% min^{-1} cm^{-2}) or RbCl (-13.88% min^{-1} cm^{-2}) was slightly different from the wild type. R228A (Table 1) had a significantly slower I_{sc} inhibition rate of -2.29% min^{-1} cm^{-2} (KCl) or -1.91% min^{-1} cm^{-2} (RbCl). Mutant toxin E235A took more than 40 min to inhibit 50% of active K^+ transport in KCl buffer. However in RbCl buffer, this mutant inhibited Rb^+ active transport in the same time (about 22 min) as the wild type. The I_{sc} inhibition rate of E235A in KCl buffer (-6.04% min^{-1} cm^{-2}) was about 4.4 times slower than the wild type. Interestingly, the measured I_{sc} inhibition rate of this mutant (-18.92% min^{-1} cm^{-2}) became similar to the wild-type toxin in buffer containing RbCl. Mutant R228K (23 min), F232Y (21 min), E235Q (25 min), and F247Y (21 min) inhibited 50% of active K^+ transport at around the same time as the wild type in KCl buffer (Figure 5, panel A). The I_{sc} inhibition rates of these mutants were not significantly different from wild type (Table 2). In RbCl buffer, R228K (37 min), F232Y (29 min), and E235Q (36 min) took longer times than wild type (22 min) to inhibit 50% of active Rb^+ transport in *M. sexta* midgut (Figure 4, panel B). The rates of I_{sc} inhibition by R228K (7.33% min^{-1} cm^{-2}), F232Y (10.23% min^{-1} cm^{-2}), and E235Q (7.39% min^{-1} cm^{-2}) were statistically different from wild type (16.8% min^{-1} cm^{-2}).

Mutant toxins R228K and E235Q were further analyzed by voltage clamp to determine the effect of these two single mutations on the maximal rate of short-circuit current inhibition (I_{sc-max}) and short-circuit current inhibition constant (K_i) of active transport of K^+ and Rb^+ in *M. sexta* midgut. Table 4 shows that the maximal rate of I_{sc} inhibition (I_{sc-max}) for E235Q (-18.35% min^{-1} cm^{-2}) is significantly reduced as compared to wild type (-50.61% min^{-1} cm^{-2}) in RbCl buffer. The I_{sc-max} of all toxins were not significantly different from each other in KCl buffer. The K_i of both R228K and E235Q toxins were also not significantly different from wild type in both KCl and RbCl buffers.

Table 4: Kinetic Parameters of Cry1Ab in the Inhibition of I_{sc} in *M. Sexta* Midgut[a]

	KCl		RbCl[b]	
toxin	K_i	I_{sc-max}	K_i	I_{sc-max}
Cry1Ab	2.83 (0.61)	54.43 (0.78)	3.64 (1.58)	50.61 (10.08)
R228K	1.31 (0.84)	31.21 (11.02)	5.98 (1.20)	33.11 (0.59)
E235Q	1.52 (0.81)	28.33 (10.25)	1.20 (0.41)	18.35 (1.79)*

[a] Each value is the average of three separate runs of voltage clamped midgut of fifth instar *M. sexta*. Values in parentheses are standard deviations. Parameters were estimated by fitting the plot of I_{sc} inhibition rates and toxin concentrations (0.1, 0.5, 1, 5, 10 nM) in 32 mM KCl or RbCl with Michaelis−Menten equation, $I_{sc} = I_{sc-max}$ [S]/[S] + K_i. K_i, short-circuit current inhibition constant (nM). I_{sc-max}, maximal rate of I_{sc} inhibition (% min^{-1} cm^2). [b] Value with asterisk is significantly different from wild type ($P < 0.05$). Means were compared by Bonferroni *t*-test.

DISCUSSION

α-Helix 7 is located in the highly conserved block 2 in domain I of Cry1Ab δ-endotoxin and is centrally located in the core of the toxin between domains I and II (*7*), Figure 1. We introduced single alanine mutations in this region to determine its structural and functional role in insecticidal activity. All charged residues and virtually all hydrophobic aromatic amino acids were mutated. The stable mutant toxins R224A, R228A, and E235A showed significantly reduced toxicity to *M. sexta* larvae (Table 1). Our attempts to introduce more alanine substitutions in α-helix 7 at other positions resulted in structural instability of the protein. The crystal structure of Cry1Aa (*7*) and the high homology of this toxin with other Cry1A toxins (*1*) allows us to propose an explanation for the instability of these mutants on the basis of the Cry1Aa structure. According to this crystal structure, α-helix 7 residues R233, R234, and D242 are involved in intramolecular salt bridges with domain II residues E288, E274, and R265, respectively. The residue W226 in α-helix 7 is buried within the domain I and domain II interface. The mutations we made in these residues in Cry1Ab could have resulted in the disruption of these interactions that led to the observed structural instability. The *M. sexta* gut juice and the Thermolysin assays suggest that residues R224, R228, and E235 are not directly involved in intramolecular interactions critical for the stability of the toxin. The SDS−PAGE analysis of protoxins treated with gut juice produced mutant activated toxins of the same molecular weight as the wild type. This result suggests that the alanine substitution at any of these three positions did not expose the folded conformation of the toxin core to further proteolytic attack during the gut juice treatment that would destroy the toxin activation process. These results are

further confirmed by the absence of spectral changes in the CD analyses of the mutant toxins. When conservative mutations were introduced in R228 and E235, toxicity was recovered. Our observations that R224, R228, and E235 are not critical for structural stability are supported by the crystallographic study (*7*). In vitro studies have shown that the activated toxin binds to receptors in susceptible lepidopteran midgut (*4*, *35*, *36*). Also, the binding of toxins to receptors in vivo has been confirmed (*37*). Our competition assay shows that the ability to compete for binding sites is comparable among R224A, R228A, and the wild type. However, a 2.5-fold increase in K_{com} (decrease in binding affinity) was observed with mutant E235A. If K_{com} can totally account for toxicity, we would expect that E235A should be the least toxic among the mutants and R224A would be as toxic as the wild type. However, our competition binding data do not show a direct correlation between K_{com} and toxicity (Table 1). Others have observed that K_{com} (called K_d in earlier work) is not correlated to toxicity (*31*, *38*). Elsewhere (*31*) we have argued that binding constants determined from competition experiments are not an accurate measure of binding affinity for Cry toxin−receptor−membrane interactions. We verified our binding results obtained from ^{125}I labeled toxins with the more sensitive SPR technique (*39*). This method has revealed a significant effect on the dissociation rate with the mutations described here (Table 3). The parameter estimates obtained from SPR study are slightly different from that obtained elsewhere (*32*) probably because of the different binding property of Cry1Ab and the higher ratio of biotin to BBMV (1:50) used than previously reported (*32*). The lack of correlation between the K_D values (Table 3) obtained from SPR and toxicity (Table 2 or given in the text) indicates a complex role for these residues in the mechanism of action. This observation has been made many times (*5*, *31*). As discussed below, we believe toxicity is more closely related to ion channel function.

One possible explanation for the loss of toxicity of these mutant toxins is the previous observation that the binding of the Bt toxin to (BBMV) quickly becomes irreversible (*31*, *35*, *36*, *38*, *39*). Irreversible binding is thought to be due to toxin insertion into the membrane, which is believed to be a prerequisite for toxicity (*31*). The amount of irreversible binding sites ($B_{max,i}$) appears to be one of the factors affecting the toxicity of R224A and R228A. If few toxins are irreversibly bound to BBMV, it is likely that the amount of toxin inducing ion-conducting pore in the membrane would also be less. When the number of functional pores induced by the toxin do not reach a threshold level, the resulting driving force needed for the inward flow of ions through these pores might not be sufficient to cancel the current produced by the electrogenic K^+ pump. Hence, R224A and R228A could not inhibit the I_{sc} in the voltage clamp assay (Figure 4, panel A) in the rate as the wild-type toxin did. The loss of I_{sc} in midguts treated with toxin is believed to be created by the large net inward flow of ions passing through the ion channels induced by the toxin. This event inhibits the K^+ pump, which causes the collapse of the transepithelial potential (*5*).

There is a direct correlation between inhibition of short circuit current for KCl (I_{sc}) and toxicity (LC_{50}), Table 1, for the mutant toxins examined in this study as shown in Figure 6. This correlation has been mentioned in several publications (*12*, *17*, *22*, *34*), but the linear correlation has not been previously presented. This correlation and the lack of direct correlation of receptor binding as K_D (Table 3) suggest an effect on toxicity downstream from the receptor binding step, that is, either membrane insertion or ion channel function.

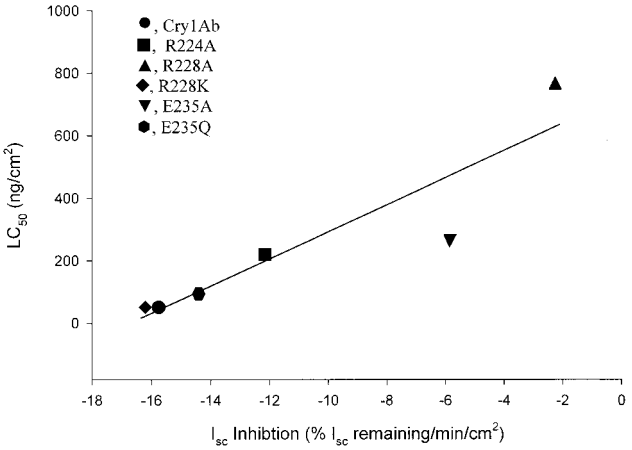

FIGURE 6: Correlation between the inhibition of short circuit current (I_{sc}) for KCl and toxicity (LC_{50}).

To explore the possibility that α-helix 7 is also involved in ion channel function we exploited the ability of *M. sexta* midgut to actively transport Rb^+ ions to determine changes in ionic permeability of the mutants. Rb^+ is the next larger alkali metal in the periodic table and might not be expected to show a significant difference in conductance across the midgut membranes. Since the permeability of untreated *M. sexta* midguts to Rb^+ is similar to K^+ (Figure 3) there should be no difference in the I_{sc} inhibition rate by the wild-type toxin in either buffer as shown in Figure 4, panels A and B. Furthermore, any observed difference in I_{sc} inhibition rate in KCl and RbCl buffer may be attributed to the mutation introduced to the Cry1Ab toxin. Comparing the I_{sc} for KCl and RbCl in Table 1, it is observed that the radical mutations (R224A, R228A, and E235A) show a correlation between I_{sc} for KCl and toxicity, while I_{sc} for RbCl is significantly different for E235A. This mutant behaves as wild type in RbCl, while it is 3-fold less active in KCl. It is tempting to speculate that the residues R224, R228, and E235 might be involved in ion channel activity, but some role of reduced receptor binding in the reduced I_{sc} cannot be discounted.

Exploring this observation further using the conservative mutant proteins (R224K, F232Y, E235Q, and F247Y), we see no loss of toxicity, binding, relative to Cry1Ab and the same level of I_{sc} in KCl (Table 2). The ability to inhibit I_{sc} in RbCl, however, is significantly reduced in three of these mutant toxins (R224K, F232Y, and E235Q). This means that despite the fact that the midgut can conduct both K^+ and Rb^+ (Figure 3), these mutant toxins recognize the difference between these cations and conduct Rb^+ about half as efficiently as K^+. We propose that these residues participate in formation of the structural pore.

We also examined the kinetic parameters of two mutant proteins (R228K and E235Q) using inhibition of I_{sc} in both KCl and RbCl (Table 4). From this analysis, we observe that the maximal rate of I_{sc} inhibition for RbCl is significantly different from KCl for E235Q. This further implicates E235 in ion channel function.

In the search for residues that are involved in ion channel function, it is necessary to anticipate the attributes of mutations in these residues. One might seek mutants that affect only ion channel function (e.g., inhibition of I_{sc} by voltage clamp) but that have no effect in structure or other known functions (e.g., binding or membrane insertion); one mutant toxin described in this study fits this criterion, E235Q under the conditions of Rb^+ conductance. On the other hand, there is no reason to believe that the key residues are only involved in a single function. If mutations such as the ones we describe here result in loss of toxicity and voltage clamp response while having a decreased affinity for receptor binding (R224A, R228A, E235A) and an unexpected increase in rate of irreversible membrane binding (R228A, E235A), they are candidates for a central role in ion channel activity. A different, and perhaps better, criteria of such a key amino acid is a clear effect on ion selectivity (R224K, F232Y, and E235Q). These mutations in α-helix 7 fit both of these criteria, making them key amino acids in the ion channel function of this toxin, similar to what has been reported recently (*21*).

ACKNOWLEDGMENT

We are grateful to David Stetson for the voltage clamp apparatus.

REFERENCES

1. Schnepf, E., Crickmore, N., Van Rie, J., Lereclus, D., Baum, J., Feitelson, J., Zeigler, D. R., and Dean, D. H. (1998) *Microbiol. Mol. Biol. Rev. 62*, 775−806.
2. Dow, J. A. T. (1986) *Adv. Insect Physiol. 19*, 187−328.
3. Choma, C., Surewicz, W., Carey, K., Poszgay, M., Raynor, T., and Kaplan, H. (1990) *Eur. J. Biochem. 189*, 523−527.
4. Van Rie, J., Jansens, S., Hofte, H., Degheele, D., and Van Mellaert, H. (1990) *Appl. Environ. Microbiol. 56*, 1378−1385.
5. Wolfersberger, M. G. (1992) *J. Exp. Biol. 172*, 377−386.
6. Crickmore, N., Zeigler, D. R., Feitelson, J., Schnepf, E., Van Rie, J., Lereclus, D., Baum, J., and Dean, D. H. (1998) *Microbiol. Mol. Biol. Rev. 62*, 807−813.
7. Grochulski, P., Masson, L., Borisova, S., Pusztai-Carey, M., Schwartz, J., Brousseau, R., and Cygler, M. (1995) *J. Mol. Biol. 254*, 447−464.
8. Li, J., Caroll, J., and Ellar, D. J. (1991) *Nature 353*, 815−821.
9. Hofte, H., and Whiteley, H. R. (1989) *Microbiol. Rev. 53*, 222−255.
10. Walters, F., Slatin, S., Kulesza, C., and English, L. (1993) *Biochem. Biophys. Res. Commun. 196*, 921−926.
11. Von Tersch, M., Slatin, S., Kulesza, C., English, L. (1994) *Appl. Environ. Microbiol. 60*, 3711−3717.
12. Chen, X. J., Lee, M. K., and Dean, D. H. (1993) *Proc. Natl. Acad. Sci. U.S.A. 90*, 9041−9045.
13. Wolfersberger, M. G., Chen, X. J., and Dean, D. H. (1996) *Appl. Environ. Microbiol. 62*, 279−282.
14. Schwartz, J. L., Potvin, L., Chen, X. L., Brousseau, R., Laprade, R., and Dean, D. H. (1997). *Appl. Environ. Microbiol. 63*, 3978−3984.
15. Wu, D., and Aronson, A. (1992) *J. Biol. Chem. 267*, 2311−2347.
16. Alzate, O. (1998) Doctoral dissertation, The Ohio State University.
17. Chen, X. J., Curtiss, A., Alcantara, E., and Dean, D. H. (1995) *J. Biol. Chem. 270*, 6412−6419.
18. Aronson, A. I., Wu, D., and Zhang, C. (1995) *J. Bact. 177*, 4059−4065.
19. Gazit, E., and Shai, Y. (1995) *J. Biol. Chem. 270*, 2571−2578.
20. Gazit, E., LaRocca, P., Sansom, M. S. P., and Shai, Y. (1998) *Proc. Natl. Acad. Sci. U.S.A. 95*, 12289−12294.
21. Chandra, A., Ghosh, P., Mandaokar, A. D., Bera, A. K., Sharma, R. P., Das, S., and Kumar, P. A. (1999) *FEBS Lett. 458*, 175−179.
22. Rajamohan, F., Alcantara, E., Lee, M. K., Chen, X. J., Curtiss, A., and Dean, D. H. (1995) *J. Bacteriol. 177*, 2276−2282.
23. Kunkel, T. (1985) *Proc. Natl. Acad. Sci. U.S.A. 82*, 488−492.
24. Sanger, F., Nicklen, S., and Coulson, A. R. (1977) *Proc. Natl. Acad. Sci. U.S.A. 74*, 5463−5467.
25. Sambrook, J., Fritsch, E. F., and Maniatis, T. (1989) *Molecular Cloning. A Laboratory Manual*, 2nd ed., Cold Spring Harbor Laboratory, Cold Spring Harbor, NY.
26. Almond, B. D., and Dean, D. H. (1993) *Appl. Environ. Microbiol. 59*, 2442−2448.
27. Laemmli, U. K., (1970) *Nature*, *227*, 680.
28. Wolfersberger, M. G., Luthy, P., Maure, A., Parenti, P., Sacchi, F., Giordana, B., and Hanozet, G. (1987) *Comp. Biochem. Biophysiol. 86A*, 301−308.
29. Lee, M. K., Milne, R. E., Ge, A. Z., and Dean, D. H. (1992) *J. Biol. Chem. 267*, 3115−3121.
30. Wu, S. J., and Dean, D. (1996) *J. Mol. Biol. 255*, 628−640.
31. Liang, Y., Patel, S. S., and Dean, D. H. (1995) *J. Biol. Chem. 270*, 24719−24724.
32. Masson, L., Mazza, A., and Brousseau, R. (1994) *Anal. Biochem. 218*, 405−412
33. Finney, D. (1972) *Statistical Method in Biological Assay*, 3rd ed., Griffin and Co., Ltd., London.
34. Liebig, B., Stetson, D. L., and Dean, D. H. (1995) *J. Insect Physiol. 41*, 17−22.
35. Hofmann, C., Luthy, P., Hutter, R., and Pliska, V. (1988) *Eur. J. Biochem. 173*, 85−91.
36. Van Rie, J., Jansens, S., Hofte, H., Degheele, D., and Van Mellaert, H. (1989) *Eur. J. Biochem. 186*, 239−247.
37. Bravo, A., Jansens, S., and Peferoen, M. (1992) *J. Invertebr. Pathol. 60*, 237−246.
38. Wolfersberger, M. G. (1990) *Experientia 46*, 475−477.
39. Phizicky, E. M., and Fields, S. (1995) *Microbiol. Rev. 59*, 94−123.
40. Stein, W. (1990) *Channels, Carriers, and Pumps: an Introduction to Membrane Transport*, Academic Press, San Diego.

BI0022240